HHS Public Access

Author manuscript

Exp Gerontol. Author manuscript; available in PMC 2019 July 15.

Published in final edited form as:

Exp Gerontol. 2018 July 15; 108: 247–255. doi:10.1016/j.exger.2018.04.024.

Effect of metabolic syndrome and aging on Ca^{2+} dysfunction in coronary smooth muscle and coronary artery disease severity in Ossabaw miniature swine

Jill K. Badin[1], **Rebecca S. Bruning**[1,2], and **Michael Sturek**[1]

[1]Department of Cellular & Integrative Physiology, Indiana University School of Medicine, Indianapolis, IN 46202-5120

[2]RTI International, Global Health Technologies, Research Triangle Park, NC 27709

Abstract

Background—Metabolic syndrome (MetS) and aging are prevalent risk factors for coronary artery disease (CAD) and contribute to the etiology of CAD, including dysregulation of Ca^{2+} handling mechanisms in coronary smooth muscle (CSM). The current study tested the hypothesis that CAD severity and CSM Ca^{2+} dysregulation were different in MetS- compared to aging-induced CAD.

Methods—Young (2.5 ± 0.2 years) and old (8.8 ± 1.2 years) Ossabaw miniature swine were fed an atherogenic diet for 11 months to induce MetS and were compared to lean age-matched controls. The metabolic profile was confirmed by body weight, plasma cholesterol and triglycerides, and intravenous glucose tolerance test. CAD was measured with intravascular ultrasound (IVUS) and histology. Intracellular Ca^{2+} ($[Ca^{2+}]_i$) was assessed with fura-2 imaging.

Results—CAD severity was similar between MetS young and lean old swine, with MetS old swine exhibiting the most severe CAD. Compared to CSM $[Ca^{2+}]_i$ handling in lean young, the MetS young and lean old swine had increased sarcoplasmic reticulum Ca^{2+} store release. MetS young swine exhibited increased Ca^{2+} influx through voltage-gated Ca^{2+} channels. Lean old swine exhibited attenuated sarco-endoplasmic reticulum Ca^{2+} ATPase activity. MetS old and MetS young swine had similar Ca^{2+} dysregulation.

Corresponding Author: Michael Sturek, M.S., Ph.D. Professor and Chair of the Department of Cellular & Integrative Physiology, Indiana University School of Medicine, 635 Barnhill Drive, MS 385, Indianapolis, IN 46202-5120, Phone: 317-274-7772, msturek@iu.edu.

Author Contributions

J.K.B and M.S. are responsible for conception and design of research; J.K.B. and R.S.B. performed experiments; J.K.B. and R.S.B. analyzed data; J.K.B. and M.S. interpreted results of experiments; J.K.B. prepared figures; J.K.B. and R.S.B. drafted manuscript; J.K.B., R.S.B., and M.S. edited and revised manuscript; J.K.B., R.S.B., and M.S. approved final version of manuscript.

Disclosures

No conflicts of interest are declared by the authors.

Conclusions—Ca^{2+} dysregulation, mainly the SR Ca^{2+} store, in CSM is more pronounced in lean old compared to both MetS groups, which is indicative of mild, proliferative CAD. MetS old and MetS young swine exhibit Ca^{2+} dysfunction that is typical of late, severe disease. The more advanced, complex plaques in MetS old swine suggest that the "aging milieu" potentiates effects of Ca^{2+} handling dysfunction in CAD.

Keywords

Atherosclerosis; obesity; metabolism; intravascular ultrasound; sarco-endoplasmic reticulum Ca^{2+} ATPase

1. Introduction

Atherosclerosis is a complex, progressive disease that develops over many years when cholesterol, fatty material, cellular waste products, fibrin, collagen, and extracellular Ca^{2+} accumulate in large and medium-sized arteries throughout the body. Coronary artery disease (CAD) is the build-up of atherosclerotic plaque in the coronary arteries leading towards occlusion and myocardial ischemia and is the leading cause of death in industrialized nations (49).

Modifiable risk factors such as physical inactivity and an unhealthy diet can potentiate metabolic changes like hypertension, dyslipidemia, obesity, insulin resistance, and glucose intolerance. Metabolic syndrome (MetS) is the clustering of 3 or more of these cardiometabolic risk factors and is associated with a 2-fold greater risk of developing CAD and a 1.6-fold increase in mortality (1, 4). However, modifiable risk factors are only part of the story. Sir William Osler, a prolific physiologist and one of the founders of Johns Hopkins University, once wrote, "A man is as old as his arteries" (57). Indeed, advancing age is one of the major non-modifiable risk factors for CAD. The prevalence of CAD increases progressively with age, and more than 50% of CAD-related deaths occur in individuals older than 75 (61, 64). The population aged 65 and older in the US is projected to double to 83.7 million by the year 2050 (20), causing a growing public health concern.

The Ossabaw miniature swine model of MetS/CAD has been well-characterized in our lab (66). These swine exhibit a "thrifty genotype" that allows them to store excess fat for later use during times of famine in their natural habitat (44, 66). In captivity, when the pigs are kept sedentary and fed a high-calorie atherogenic diet, they reliably develop all the risk factors associated with MetS in addition to diffuse atheroma and coronary artery calcification (CAC), making them a clinically relevant animal model of human MetS and subsequent CAD/CAC (17, 41, 50, 51, 54, 60, 73).

Ca^{2+} is vital to vascular smooth muscle function, as cytosolic Ca^{2+} levels regulate various cellular functions including contraction (35, 58), proliferation (33, 42, 56, 58), migration (48, 59), and transcription (30, 71). Previous research (reviewed in (65)) has identified several functional alterations in Ca^{2+} handling mechanisms associated with metabolic disorders (MetS, diabetes, dyslipidemia) that induce CAD. Ca^{2+} is an important secondary messenger that influences several physiological processes, and impairments in intracellular

Ca^{2+} handling due to dysfunction of Ca^{2+} transporter proteins and altered storage in organelles changes CSM activity and contributes to CAD etiology (28, 42, 50, 65).

Age-related alterations in intracellular Ca^{2+} regulation depend heavily on the tissue, animal, and co-existing disease states (11). These heterogeneous patterns of Ca^{2+} dysregulation are similar to the heterogeneity of metabolic dysfunction (65). There is a paucity of data regarding age-related alterations in Ca^{2+} regulation in coronary smooth muscle (CSM), which would precede extracellular CAC, an event that has been extensively documented in aging (64). The pathophysiology of MetS- and aging-induced atherosclerotic disease may be different; however, MetS-induced and aging-induced atherosclerotic CAD and the associated alterations in CSM intracellular Ca^{2+} signaling have yet to be compared directly. Therefore, the aims of the present study were to examine how modifiable (MetS) and non-modifiable (advancing age) risk factors affect 1) coronary atherosclerosis progression and 2) CSM $[Ca^{2+}]_i$ regulation. We hypothesized that CAD severity and CSM Ca^{2+} dysregulation would be different in MetS- compared to aging-induced CAD.

2. Materials and Methods

2.1. Animals

All experimental procedures involving animals were approved by the Institutional Animal Care and Use Committee at Indiana University School of Medicine with the recommendations outlined in the Guide for the Care and Use of Laboratory Animals and the American Veterinary Medical Association Panel on Euthanasia (2, 34). Ossabaw miniature swine were separated into four groups based on age and diet: lean young, MetS young, lean old, and MetS old swine (Table 1). The average age of each group can be seen in Table 1. Ossabaw swine are sexually mature by the time they reach 6 months old and can live up to 8 years in the wild and 15 years in captivity (5, 75). While there is not a linear relationship between swine and human age, swine age about 5–7 years (depending on the breed) for every 1 human year (36). Based on this conversion and the age of sexual maturity, we can estimate that the young groups of swine correlate to about 24 human years and the old groups of swine correlate to about 63 human years. These old swine are medically relevant, as the average age of patients who experience their first myocardial infarction is 60 years (37). Both lean groups were fed 725 g/day of regular chow (5L80, Purina Test Diet, Richmond, IN) that contained 18% kcal from protein, 71% kcal from complex carbohydrates, and 11% kcal from fat. To induce MetS, swine in both MetS groups were fed 1000 g/day of an excess-calorie, atherogenic diet for 11 months (KT324, Purina Test Diet, Richmond, IN) that provided 16.3% kcal from protein, 40.8% kcal from complex carbohydrates, 19% kcal from fructose, and 42.9% kcal from fat. Fat calories were derived from a mixture of lard, hydrogenated soybean oil, and hydrogenated coconut oil and was supplemented with 2.0% cholesterol and 0.7% sodium cholate by weight. All animals had free access to drinking water.

2.2. Intravenous glucose tolerance testing

Prior to intravenous glucose tolerance testing (IVGTT), conscious swine were acclimatized to low-stress restraint in a sling. The pigs fasted overnight before an IVGTT and fasting

baseline blood samples were obtained. Glucose (1 g/kg body weight, IV) was administered and timed blood samples were collected as previously described by our laboratory (17, 54, 66) for blood glucose measurements (YSI 2300 STAT Plus Glucose analyzer, YSI Life Sciences, Yellow Springs, OH).

2.3. Metabolic phenotyping

Blood samples were obtained before euthanasia and triglycerides, total cholesterol, and blood chemistry profiles were assessed (Antech Diagnostics, West Lafayette, IN). Blood pressure measurements were attained while swine were under anesthesia with isoflurane.

2.4. Intravascular ultrasound

Swine were anesthetized with isoflurane (2 to 6%) and intravascular ultrasound (IVUS) was performed as previously described (52, 54, 66). Briefly, after an overnight fast swine were anesthetized via intramuscular injection of 2.2 mg/kg xylazine and 5.5 mg/kg Telazol (Fort Dodge Animal Health, Fort Dodge, IA). Swine were intubated and anesthesia was maintained with 2 to 4% isoflurane in 100% O_2. The isoflurane level was adjusted to maintain anesthesia with stable hemodynamics. Heart rate, aortic blood pressure, respiratory rate, and electrocardiographic data were continuously monitored throughout the procedure (GE Dash 4000, General Electric, Boston, MA). Following a right femoral artery cut-down, a 7 F introducer sheath was inserted for access and heparin was administered (200 U/kg). Next, a 7 F guiding catheter (Amplatz L, Cordis, Bridgewater, NJ) was advanced to the left main coronary ostium. A 3.2 F, 45 MHz VUS catheter (Revolution, Volcano, Corp., Rancho Cordova, CA) was advanced over a percutaneous transluminal coronary angioplasty guide wire and positioned in the left anterior descending (LAD) artery. Automated IVUS pullback was performed and recorded at 0.5 mm/sec and 30 frames/second. Pigs were euthanized after the IVUS procedure via cardiectomy and coronary arteries were removed for further analysis. Still frame IVUS pullback images were obtained offline at 1 mm intervals. Percent wall coverage and percent plaque burden were obtained using Image J software (1.48v, National Institutes of Health, USA).

2.5. Assessment of $[Ca^{2+}]_i$ regulation

Whole-cell intracellular free Ca^{2+} levels were measured at room temperature (22 to 25 °C) by using the fluorescent Ca^{2+} indicator fura-2 AM (InCa++ Ca2+ Imaging System, Intracellular Imaging, Cincinnati, OH) as previously described (28, 31, 54, 74). Briefly, freshly dispersed smooth muscle cells from the LAD were incubated with 3.0 μM fura-2 AM (Molecular Probes, Eugene, OR) in a shaking water bath at 37 °C for 45 min before being washed in a solution containing low Ca^{2+} concentration. An aliquot of cells loaded with fura-2 AM was placed on a coverslip contained within a constant-flow superfusion chamber that was mounted on an inverted epifluorescent microscope (model TMS-F, Nikon, Melville, NY), with flow maintained at a constant rate of 1–2 mL/min. Basal Ca^{2+} levels were measured in physiologic salt solution composed of the following (in mM): 2 $CaCl_2$, 138 NaCl, 1 $MgCl_2$, 5 KCl, 10 HEPES, 10 glucose; pH 7.4. Calcium influx and maximal sarcoplasmic reticulum (SR) Ca^{2+} loading was accomplished by depolarization with high (80 mM) K^+ solution (2 $CaCl_2$, 63 NaCl, 1 MgCl, 80 KCl, 10 HEPES, 10 glucose; pH 7.4) (54). SR Ca^{2+} stores were released with 5 mM caffeine in Ca^{2+}- free solution (138 NaCl, 1

$MgCl_2$, 5 KCl, 10 HEPES, 10^{-5} M K^+-EGTA, 10 glucose; pH 7.4). A caffeine wash-out phase was used to determine sarco-endoplasmic reticulum Ca^{2+} ATPase (SERCA) function via the undershoot below baseline during this recovery period (13, 50, 62). The increased $[Ca^{2+}]_i$ after caffeine exposure stimulates Ca^{2+} extrusion, allowing $[Ca^{2+}]_i$ to equilibrate to baseline levels (3). However, SERCA is also stimulated by high $[Ca^{2+}]_i$ and low concentrations of Ca^{2+} inside the SR after caffeine exposure (3, 77). As the SR initially accumulates Ca^{2+} quicker than Ca^{2+} can enter the cell, the signal drops below baseline (the "undershoot") (3). Furthermore, application of the SERCA inhibitor cyclopiazonic acid abolishes this undershoot (3). Therefore, SERCA function is directly responsible for the undershoot below baseline (3, 22, 77). Voltage-gated calcium channel (VGCC) activity was determined by measuring barium influx during superfusion with a high (2 mM) Ba^{2+} solution (2 $BaCl_2$, 63 NaCl, 1 $MgCl_2$, 80 KCl, 10 HEPES, 10 glucose; pH 7.4), which contained low Na^+ (5 mM Na^+) in order to limit Ba^{2+} extrusion through the sodium-calcium exchanger (solution labelled as "2Ba80K5Na" in Fig. 4B) (28). Fura-2 in CSM was excited by light from a 300 W xenon arc lamp that was passed through a computer-controlled filter changer containing 340 nm and 380 nm bandpass filters every 0.30 and 0.05 seconds, respectively. The fluorescence emission at 510 nm was collected by using a monochrome charge-coupled device camera (COHU, San Diego, CA). Whole-cell fura-2 fluorescence was expressed as the 340 nm/380 nm ratio of fura-2 emission. Graphs demonstrating the experimental protocols are shown in Figs. 3A and 3B.

2.6. Histology

Coronary artery segments were collected at euthanasia and fixed in 10% phosphate buffered formalin for 24 hours before being switched to 70% ethanol solution. Samples were paraffin embedded, sectioned (5 μm thick), mounted on a slide and stained by the Indiana University Histology Core (Indiana University School of Medicine, Indianapolis, IN). Verhoeff-Van Gieson (VVG) elastin staining was performed to determine the location of the external elastic lamina (EEL) and the internal elastic lamina (IEL) to assess wall thickness, medial area, and the intima/media ratio as measures of atherosclerosis progression (50, 54). Wall thickening (percent media plus percent neointima) was measured by the following equation:

$$\left[\left(\frac{Area\ within\ EEL - Area\ within\ IEL}{Area\ within\ EEL}\right) + \left(\frac{Area\ within\ IEL - Area\ of\ Lumen}{Area\ within\ EEL}\right)\right] \times 100\,\%$$

The media area was calculated as the area within the EEL minus the area within the IEL. The intima area was calculated as the area within the IEL minus the area of the lumen. All images were captured with a Leica DM3000 microscope connected to Leica Application Suites V4.1 software (Leica Microsystems GmbH, Wetzlar, Germany) and analyzed using (Adobe Photoshop® CS6).

2.7. Statistics

Statistical analysis was performed using GraphPad Prism 5.0 (San Diego, CA). One-way analysis of variance (ANOVA) with Tukey post hoc analysis and two-way ANOVA with Bonferroni post hoc analysis were performed when appropriate. Data are represented as mean ± SEM and $p < 0.05$ was considered statistically significant.

3. Results

3.1. Ossabaw Swine Cardiometabolic Characteristics

The experimental groups' cardiometabolic characteristics are presented in Table 1. The Ossabaw swine were separated by age and metabolic profile. Lean old swine were shown to be healthy, as indicated by their body weight, cholesterol, triglycerides, and blood glucose measurements derived from the IVGTT assessment. Our laboratory and others have extensively characterized cardiometabolic profiles in Ossabaw swine fed regular chow diets and hypercaloric, atherogenic diets to induce MetS (13, 27, 44, 51, 52, 54, 55, 69). MetS was confirmed in the MetS young and MetS old swine groups, both of which developed obesity, hypercholesterolemia, and elevated peak glucose and area under the curve during IVGTTs (52, 54). Blood pressure measurements were not significantly different between groups (data not shown) and were taken while swine were anaesthetized. The lean old swine had significantly lower serum triglycerides and fasting blood glucose, which is characteristic of older swine (39, 70).

3.2. Histological Assessment of Vascular Health

Atherosclerosis progression was assessed by VVG staining in the proximal right coronary arteries (Fig. 1A–D) that enabled measurement of wall thickness (%media + %neointima), media thickness, and intima:media ratio (Fig. 1E–G). Both advanced age and MetS independently caused swine to exhibit elevated wall thickening, with MetS old swine exhibiting significantly greater wall thickening than the other three groups (Fig. 1E). Media thickness was elevated in the MetS young and lean old swine compared to the lean young swine group swine (Fig. 1F). To determine whether this change was due mainly to media thickening, which is characteristic of aging (63, 76), or intimal thickening, which is characteristic of CAD (63), the intima:media area ratio was assessed (Fig. 1G). The MetS young swine trended towards a higher intima:media ratio, but the MetS old swine had a significantly higher intima:media ratio, indicating that a bulk of the wall thickening in both MetS groups was due to neointimal thickening while the wall thickening in the lean old swine was due to medial thickening.

3.3. IVUS Assessment of Coronary Plaque Severity

After angiography was employed to locate the LAD and circumflex (CFX) arteries for catheter placement (Fig. 2A), cross-sectional images of the arteries were taken using an IVUS catheter (representative IVUS still frames in Fig. 2B–C). Unfortunately, 2 out of the 3 MetS old swine died on the operating table before IVUS could be recorded, so this group was not included in the IVUS analyses. Percent wall coverage increased in MetS young swine (Fig. 2D) and percent plaque burden increased in both MetS young and lean old swine compared to lean young swine (Fig. 2E). These data suggest that MetS young swine and lean old swine have similar disease severities.

3.4. Correlation of percent wall coverage and percent plaque burden with age

Percent wall coverage (Fig. 2F) and percent plaque burden (Fig. 2G) of the lean young and lean old swine were plotted against age of the individual pig. Analysis revealed that both

percent wall coverage and plaque burden are positively correlated with age. This supports the notion that CAD severity increases with age and that older individuals are more at risk for atherosclerotic vessel occlusion.

3.5. Assessment of the Effects of MetS and Advancing Age on CSM cell $[Ca^{2+}]_i$

Figure 3A–B shows a representative CSM $[Ca^{2+}]_i$ response from a cell isolated from a lean young swine. When we assessed the caffeine-sensitive SR store release in the absence of extracellular Ca^{2+} to measure the SR storage capacity, we observed that the MetS young swine had an elevated SR store that was even higher in the lean old swine compared with the lean young group (Fig. 3C). When we measured the undershoot after SR store release in the absence of extracellular Ca^{2+} to get an index of SERCA activity (3, 22, 77), we observed that the MetS young and lean old swine had an attenuated undershoot compared with the lean young swine (Fig. 3D). VGCC activity was assessed using a solution high in K^+ (80 mM K^+) to activate VGCC, low in Na^+ (5 mM Na^+) to inhibit the sodium-calcium exchanger, and high in Ba^{2+} (2 mM Ba^{2+}), which enters the CSM exclusively via VGCC and binds to fura-2 (28). CSM cells from MetS young and lean old swine exhibited an increased Ba^{2+} influx rate compared with the lean young swine group (Fig. 3E).

4. Discussion

Cytosolic Ca^{2+} is a primary regulator of contraction and phenotypic modulation of CSM, which plays an integral role in atherosclerosis pathology and has been reviewed elsewhere (58, 65). MetS- and aging-induced changes of the structure of the vascular have been well documented, but CSM Ca^{2+} dysregulation in MetS- and age-induced CAD have never been directly compared in swine.

This study characterized aging-related CSM Ca^{2+} dysregulation and provides insight into the disease characteristics of two common etiologies of atherosclerosis. We show for the first time that, although MetS-induced CAD and aging occlude the arteries to a similar degree in our swine model, the Ca^{2+} handling mechanisms present in lean old swine are exaggerated compared with MetS-induced CAD. This indicates that MetS young swine have CSM Ca^{2+} dysregulation that mirrors severe disease and lean old swine have CSM Ca^{2+} dysregulation that mirrors mild disease (50).

Our laboratory has explored changes in Ca^{2+} handling in CSM throughout the time-course of CAD progression in Ossabaw swine from healthy, lean pigs to obese, MetS pigs with advanced calcified CAD lesions. “Early stages” of CAD were characterized by pigs on the same atherogenic diet used in the present study for 6 to 9 months, while “later stages” of CAD were defined by pigs on an atherogenic diet for approximately 12 months (50). *In vivo* assessment of atherosclerosis confirmed greater CAD burden in those pigs fed an atherogenic diet for a longer duration (50). Interestingly, Ca^{2+} influx after membrane depolarization with 80 mM K^+ and caffeine-sensitive SR store-release was exaggerated in early CAD, which began to decline in later stages of CAD (50). The MetS old swine had similar Ca^{2+} dysregulation as the MetS young swine, but a much greater wall thickness and neointima formation. Taken together, this data suggests vascular changes with aging accelerate disease progression.

Specific Ca^{2+} handling dysfunction is associated with certain structural changes in the arterial wall. For example, increased SR Ca^{2+} store has been implicated with CSM proliferation and wall thickening (25, 46, 65). In the present study, we show that lean young swine and MetS old swine have similar medial thickness (Fig. 1F), which is reflected in their comparable SR Ca^{2+} store release capacities (Fig. 3C). This could be due to the decreased proliferative ability of CSM cells or an increase in apoptotic CSM cells in MetS old swine (53, 79). MetS young swine have elevated media thickness that is related to their elevated SR Ca^{2+} store release and lean old swine had even more elevated media thickness and associated SR Ca^{2+} store release. Future studies are needed to address how functional alterations in Ca^{2+} handling mechanisms cause age and metabolic-induced structural changes in CSM.

There are numerous other channels involved in Ca^{2+} homeostasis in CSM that we have not investigated in the present study. For example, VGCCs are not the only Ca^{2+} influx mechanisms present on CSM cell membranes. Transient receptor potential canonical (TRPC) channels are ligand-gated channels that also cause Ca^{2+} influx (65). TRPC channel functional alterations have also been implicated in both MetS (65, 74) and aging (18, 38). There is an increase in TRPC channel function in Ossabaw swine with MetS that is reversed with exercise (65, 74) and an increase in TRPC channel expression in aged rat myocardium (38). However, another study in aged rat aorta smooth muscle found that different TRPC isoforms are differentially upregulated and downregulated in aging, further complicating this relationship (18). Future studies will be needed to address TRPC channel activity in MetS and aging.

Ca^{2+} sequestration can also be accomplished by the mitochondria, and mitochondrial Ca^{2+} buffering has also been shown to undergo changes associated with MetS and aging (7, 10). Under physiological conditions, the Ca^{2+} uniporter, which is driven by the concentration gradient and the membrane potential, is responsible for mitochondrial Ca^{2+} uptake. However, respiratory chain dysfunction as a result of MetS or aging causes the loss of mitochondrial membrane potential, leading to reduced uniporter function and increased $[Ca^{2+}]_i$ (76, 78). Studies in rat models of aging have conflicting results, with some showing decreased mitochondrial Ca^{2+} sequestration (43) and some showing increased Ca^{2+} stores (47). Clearly, more studies in clinically relevant animal models are needed to elucidate the effects of both age and MetS on mitochondrial Ca^{2+} sequestration to paint a better picture of whole-cell calcium handling in these states.

Endothelial dysfunction is thought to be an initial step in arteriosclerosis and atherogenesis (40). In both MetS and aging, nitric oxide bioavailability decreases and reactivity to the vasoconstrictor endothelin increases, potentially causing impaired coronary blood flow control (14, 23, 40, 67). Furthermore, aging results in significant oxidative stress which can cause NOS isoforms to produce vasoconstriction instead of vasodilation due to eNOS uncoupling, loss of cofactor (BH4) and formation of peroxynitrate from NO and free radical interaction (14). This not only reduces NO vasodilation but can cause vasoconstriction resulting in more turbulent flow, which is one of the initial events of atherogenesis (14, 76). Endothelial function was not assessed in the scope of this study, but this provides a potential direction for future studies.

Aging-induced changes in Ca^{2+} handling in smooth muscle vary depending on tissue bed and species (11). Although cardiac events are the leading cause of death in aged individuals (49), there is a paucity of literature about the effects of age on CSM Ca^{2+} handling despite its structural and functional importance. We fill that gap of knowledge by demonstrating that swine with MetS exhibit Ca^{2+} dysfunction that is characteristic of severe CAD regardless of the age of the animal, and lean old swine exhibit Ca^{2+} dysfunction that is characteristic of mild CAD. The lean old swine have increased SR Ca^{2+} store, increased VGCC activity, and decreased SERCA function in CSM (Fig. 4C–E).

While the short maturation time and lifespan of rodents and rabbits makes them tempting to use in aging studies, their size and cardiovascular anatomy brings their clinical relevance into question (45). However, because of their anatomy and physiology, the Ossabaw swine are a far more superior model than rodents or rabbits (29). However, due to cost, space, and time limitations, Ossabaw swine have not previously been used in an aging study. This truly unique study compared CSM Ca^{2+} dysfunction in lean young, MetS young, lean old, and MetS old swine, a feat never before published due to the long lifespan of swine and cost of maintaining pigs until they reach an advanced age.

Aging and atherosclerosis are likely not mutually exclusive - atherosclerosis causes premature and accelerated vascular aging and, conversely, vascular aging promotes atherosclerosis (72). The concept that MetS accelerates vascular aging is supported in this study. Even though plaque severity (medial area) was comparable between the MetS young and lean old group (Fig. 2D–E), the MetS young swine exhibited Ca^{2+} dysfunction that was on par with more severe CAD (Fig. 3C–E) (50). In fact, the Ca^{2+} dysfunction exhibited by the MetS young swine more closely resembled that of MetS old swine as opposed to the lean young swine, indicating that the presence of MetS causes Ca^{2+} dysregulation that is typical of severe CAD regardless of the actual age of the individual animal. It is notable also that the plaque was more complex (necrotic core, intimal lesions) in young and old MetS. Lean old swine exhibited Ca^{2+} dysfunction that is characteristic of mild disease, where Ca^{2+} signaling is enhanced (Fig. 3C–E) (50).

The similarities in Ca^{2+} dysfunction, but differences in plaque severity, between the MetS young and MetS old swine brings forth the possibility that the aging milieu predisposes individuals to exhibit accelerated plaque growth. Indeed, age has been associated with dyslipidemia (12), oxidative stress (24), insulin resistance (16), hypertension (24), and inflammation (9). These, along with increased cellular senescence, which has been shown to play a part in atherosclerotic progression at all stages of the disease and is associated with advanced atherosclerotic plaques (8), comprise a perfect storm for plaque progression, and could cause plaques to develop more rapidly after Ca^{2+} dysfunction develops.

Dyslipidemia, particularly elevated levels of LDL-cholesterol (LDL-C) is a strong individual risk factor predicting coronary artery disease progression (32). Cumulative LDL exposure over a lifetime will be higher in older individuals and results in a greater risk of CAD development and progression (32). This could explain why the lean old swine have similar wall thickness and plaque burden compared to MetS young swine even though the lean old swine had significantly lower cholesterol levels at time of sampling (Table 1). This

cumulative LDL exposure could be considered a part of the aging milieu that contributes to accelerated CAD progression.

A few limitations of this study were the sex differences between groups and lack of characterization of the sex hormone profile. The two MetS groups only contained female swine, while the two lean groups contained both female and castrated male swine (Table 1). Estrogen has been shown to be vasoprotective in the coronary circulation in several studies (15, 26, 68), while testosterone has been shown to be harmful in the context of the coronary circulation (19, 68). However, castrated male and intact female Yucatan swine have similar serum testosterone levels (6) and intact female dogs have similar estradiol levels as neutered males (21). While the current study did not include serum estrogen levels of all the swine, the literature supports the hypothesis that castrated males and intact females have a similar sex hormone profile However, hormonal deficiency in menopausal women is associated with arterial stiffness and associated with the rise in cardiovascular diseases, but cannot be assessed in the current study (72). Another limitation of this study was the small sample size, especially in regard to the MetS old swine group. Future studies will need to employ a higher sample size to ensure statistical significance.

We report here that MetS young and lean old swine have similar elevated plaque burden and wall thickening due to media remodeling, while MetS old swine have even greater wall thickening due to neointima formation. However, the Ca^{2+} dysfunction seen in MetS young and MetS old swine follow a similar pattern as that seen in severe CAD. Lean old swine have Ca^{2+} dysfunction that is indicative of mild disease. These data point to the possibility that, although Ca^{2+} handling is similar in a younger animal with less overt disease, the aging milieu can cause more advanced coronary plaques to develop in the context of MetS.

Acknowledgments

Funding

This research was supported by HL125385, P30 DK097512, T32 HL079995, Indiana University School of Medicine Center of Excellence in Cardiovascular Research, and the Fortune-Fry Ultrasound Research Fund.

We are grateful for the technical assistance of James P. Byrd, Dr. Mouhamad Alloosh, Ayeeshik Kole, and Dr. Stacey Dineen-Rodenbeck. We would like to thank the Indiana University School of Medicine Histology Core (Dr. Keith Condon) for processing the histology and use of their equipment and Dr. Robert Considine's laboratory for performing the insulin assays (P30 DK097512).

Abbreviations

$[Ca^{2+}]_i$	intracellular free calcium
CAD	coronary artery disease
CAC	coronary artery calcification
Cfx	circumflex artery
CSM	coronary smooth muscle
EEL	external elastic lamina

IEL	internal elastic lamina
IVGTT	intravenous glucose tolerance test
IVUS	intravascular ultrasound
LAD	left anterior descending artery
MAP	mean arterial pressure
MetS	metabolic syndrome
SERCA	sarco-endoplasmic reticulum Ca^{2+} ATPase
SR	sarcoplasmic reticulum
VGCC	voltage-gated calcium channel
VVG	Verhoeff-van Gieson

References

1. Aird WC. Phenotypic heterogeneity of the endothelium: I. Structure, function, and mechanisms. Circ Res. 2007; 100:158–173. [PubMed: 17272818]
2. AVMA Panel on Euthanasia. American Veterinary Medical Association. 2000 Report of the AVMA panel on euthanasia. JAVMA. 2001; 218:669–696. [PubMed: 11280396]
3. Baro I, O'Neill SC, Eisner DA. Changes of intracellular [Ca2+] during refilling of sarcoplasmic reticulum in rat ventricular and vascular smooth muscle. J Physiol. 1993; 465:21–41. [PubMed: 8229834]
4. Berger JS, Hochman J, Lobach I, Adelman MA, Riles TS, Rockman CB. Modifiable risk factor burden and the prevalence of peripheral artery disease in different vascular territories. J Vasc Surg. 2013; 58:673–681. e671. [PubMed: 23642926]
5. Bollen, PJA., Hansen, AK., Alstrup, AKO. The laboratory animal pocket reference series. Boca Raton, FL: CRC Press/Taylor & Francis; 2010. Important Biological Features; p. 1-14.
6. Bowles DK, Heaps CL, Turk JR, Maddali KK, Price EM. Hypercholesterolemia inhibits L-type calcium current in coronary macro-, not microcirculation. J Appl Physiol. 2004; 96:2240–2248. [PubMed: 14752123]
7. Camello-Almaraz C, Gomez-Pinilla PJ, Pozo MJ, Camello PJ. Mitochondrial reactive oxygen species and Ca2+ signaling. Am J Physiol Cell Physiol. 2006; 291:C1082–1088. [PubMed: 16760264]
8. Childs BG, Baker DJ, Wijshake T, Conover CA, Campisi J, van Deursen JM. Senescent intimal foam cells are deleterious at all stages of atherosclerosis. Science. 2016; 354:472–477. [PubMed: 27789842]
9. Chung HY, Cesari M, Anton S, Marzetti E, Giovannini S, Seo AY, Carter C, Yu BP, Leeuwenburgh C. Molecular inflammation: underpinnings of aging and age-related diseases. Ageing research reviews. 2009; 8:18–30. [PubMed: 18692159]
10. Csordas G, Hajnoczky G. SR/ER-mitochondrial local communication: calcium and ROS. Biochim Biophys Acta. 2009; 1787:1352–1362. [PubMed: 19527680]
11. Decuypere JP, Monaco G, Missiaen L, De Smedt H, Parys JB, Bultynck G. IP(3) Receptors, Mitochondria, and Ca Signaling: Implications for Aging. Journal of aging research. 2011; 2011:920178. [PubMed: 21423550]
12. LEC DG, Cogger VC, McCuskey RS, RDEC, Smedsrod B, Sorensen KK, Warren A, Fraser R. Age-related changes in the liver sinusoidal endothelium: a mechanism for dyslipidemia. Ann N Y Acad Sci. 2007; 1114:79–87. [PubMed: 17804522]

13. Dineen SL, McKenney ML, Bell LN, Fullenkamp AM, Schultz KA, Alloosh M, Chalasani N, Sturek M. Metabolic Syndrome Abolishes Glucagon-Like Peptide 1 Receptor Agonist Stimulation of SERCA in Coronary Smooth Muscle. Diabetes. 2015; 64:3321–3327. [PubMed: 25845661]
14. Donato AJ, Morgan RG, Walker AE, Lesniewski LA. Cellular and molecular biology of aging endothelial cells. J Mol Cell Cardiol. 2015; 89:122–135. [PubMed: 25655936]
15. Dubey RK, Jackson EK, Keller PJ, Imthurn B, Rosselli M. Estradiol metabolites inhibit endothelin synthesis by an estrogen receptor-independent mechanism. Hypertension. 2001; 37:640–644. [PubMed: 11230349]
16. Dubowitz N, Xue W, Long Q, Ownby JG, Olson DE, Barb D, Rhee MK, Mohan AV, Watson-Williams PI, Jackson SL, Tomolo AM, Johnson TM 2nd, Phillips LS. Aging is associated with increased HbA1c levels, independently of glucose levels and insulin resistance, and also with decreased HbA1c diagnostic specificity. Diabet Med. 2014; 31:927–935. [PubMed: 24698119]
17. Dyson MC, Alloosh M, Vuchetich JP, Mokelke EA, Sturek M. Components of metabolic syndrome and coronary artery disease in female Ossabaw swine fed excess atherogenic diet. Comp Med. 2006; 56:35–45. [PubMed: 16521858]
18. Erac Y, Selli C, Kosova B, Akcali KC, Tosun M. Expression levels of TRPC1 and TRPC6 ion channels are reciprocally altered in aging rat aorta: implications for age-related vasospastic disorders. Age. 2010; 32:223–230. [PubMed: 20431989]
19. Farhat MY, Wolfe R, Vargas R, Foegh ML, Ramwell PW. Effect of testosterone treatment on vasoconstrictor response of left anterior descending coronary artery in male and female pigs. J Cardiovasc Pharmacol. 1995; 25:495–500. [PubMed: 7769819]
20. Forman DE, Alexander K, Brindis RG, Curtis AB, Maurer M, Rich MW, Sperling L, Wenger NK. Improved Cardiovascular Disease Outcomes in Older Adults. F1000 Research. 2016; 5
21. Frank LA, Rohrbach BW, Bailey EM, West JR, Oliver JW. Steroid hormone concentration profiles in healthy intact and neutered dogs before and after cosyntropin administration. Domest Anim Endocrinol. 2003; 24:43–57. [PubMed: 12450624]
22. Ganitkevich VY, Isenberg G. Caffeine-induced release and reuptake of Ca^{2+} by Ca^{2+} stores in myocytes from guinea-pig urinary bladder. J Physiol(Lond). 1992; 458:99–117. [PubMed: 1284569]
23. Gerhard M, Roddy MA, Creager SJ, Creager MA. Aging progressively impairs endothelium-dependent vasodilation in forearm resistance vessels of humans. Hypertension. 1996; 27:849–853. [PubMed: 8613259]
24. Ghebre YT, Yakubov E, Wong WT, Krishnamurthy P, Sayed N, Sikora AG, Bonnen MD. Vascular Aging: Implications for Cardiovascular Disease and Therapy. Translational medicine. 2016; 6
25. Ghosh TK, Bian JH, Short AD, Rybak SL, Gill DL. Persistent intracellular calcium pool depletion by thapsigargin and its influence on cell growth. J Biol Chem. 1991; 266:24690–24697. [PubMed: 1761564]
26. Han S-Z, Karaki H, Ouchi Y, Akishita M, Orimo H. 17β-estradiol inhibits Ca^{2+} influx and Ca^{2+} release induced by thromboxane A_2 in porcine coronary artery. Circulation. 1995; 91:2619–2626. [PubMed: 7743625]
27. Handa RK, Liu Z, Connors BA, Alloosh M, Basile DP, Tune JD, Sturek M, Evan AP, Lingeman JE. Effect of renal shock wave lithotripsy on the development of metabolic syndrome in a juvenile swine model: a pilot study. J Urol. 2015; 193:1409–1416. [PubMed: 25245490]
28. Heaps CL, Sturek M, Price EM, Laughlin MH, Parker JL. Sarcoplasmic reticulum Ca(2+) uptake is impaired in coronary smooth muscle distal to coronary occlusion. Am J Physiol Heart Circ Physiol. 2001; 281:H223–H231. [PubMed: 11406489]
29. Heinonen, IHA., Sorop, O., Merkus, D., Duncker, DJ. Comparative Physiology and Pathophysiology of the Coronary Circulation. In: Escaned, J., Davies, J., editors. Physiological assessment of coronary stenoses and the microcirculation. London: Springer; 2017. p. 287-294.
30. Hill-Eubanks DC, Werner ME, Heppner TJ, Nelson MT. Calcium signaling in smooth muscle. Cold Spring Harb Perspect Biol. 2011; 3:a004549. [PubMed: 21709182]
31. Hill BJF, Katwa LC, Wamhoff BR, Sturek M. Enhanced endothelin(A) receptor-mediated calcium mobilization and contraction in organ cultured porcine coronary arteries. J Pharmacol Exp Ther. 2000; 295:484–491. [PubMed: 11046079]

32. Horton JD, Cohen JC, Hobbs HH. PCSK9: a convertase that coordinates LDL catabolism. J Lipid Res. 2009; 50(Suppl):S172–S177. [PubMed: 19020338]
33. House SJ, Potier M, Bisaillon J, Singer HA, Trebak M. The non-excitable smooth muscle: calcium signaling and phenotypic switching during vascular disease. Pflugers Arch. 2008; 456:769–785. [PubMed: 18365243]
34. Institute for Laboratory Animal Research. Guide for the care and use of laboratory animals. Washington, D.C: National Academy Press; 2010.
35. Jiang H, Stephens NL. Calcium and smooth muscle contraction. Mol Cell Biochem. 1994; 135:1–9. [PubMed: 7816050]
36. Jin L, Jiang Z, Xia Y, Lou P, Chen L, Wang H, Bai L, Xie Y, Liu Y, Li W, Zhong B, Shen J, Jiang A, Zhu L, Wang J, Li X, Li M. Genome-wide DNA methylation changes in skeletal muscle between young and middle-aged pigs. BMC Genomics. 2014; 15:653. [PubMed: 25096499]
37. Kapadia S. Trends in cardiovascular risk profiles. Cleve Clin J Med. 2017; 84:e6–e9. [PubMed: 29281605]
38. Kaplan P, Jurkovicova D, Babusikova E, Hudecova S, Racay P, Sirova M, Lehotsky J, Drgova A, Dobrota D, Krizanova O. Effect of aging on the expression of intracellular Ca(2+) transport proteins in a rat heart. Mol Cell Biochem. 2007; 301:219–226. [PubMed: 17549608]
39. Kawaguchi H, Yamada T, Miura N, Noguchi M, Izumi H, Miyoshi N, Tanimoto A. Sex differences of serum lipid profile in novel microminipigs. In Vivo. 2013; 27:617–621. [PubMed: 23988896]
40. Knudson JD, Dincer UD, Bratz IN, Sturek M, Dick GM, Tune JD. Mechanisms of coronary dysfunction in obesity and insulin resistance. Microcirculation. 2007; 14:317–338. [PubMed: 17613805]
41. Kreutz RP, Alloosh M, Mansour K, Neeb Z, Kreutz Y, Flockhart DA, Sturek M. Morbid obesity and metabolic syndrome in Ossabaw miniature swine are associated with increased platelet reactivity. Diabetes Metab Syndr Obes. 2011; 4:99–105. [PubMed: 21660293]
42. Kruse HJ, Bauriedel G, Heimerl J, Hofling B, Weber PC. Role of L-type calcium channels on stimulated calcium influx and on proliferative activity of human coronary smooth muscle cells. J Cardiovasc Pharmacol. 1994; 24:328–335. [PubMed: 7526069]
43. Lakatta EG. Arterial and cardiac aging: major shareholders in cardiovascular disease enterprises: Part III: cellular and molecular clues to heart and arterial aging. Circulation. 2003; 107:490–497. [PubMed: 12551876]
44. Lee L, Alloosh M, Saxena R, Van Alstine W, Watkins BA, Klaunig JE, Sturek M, Chalasani N. Nutritional model of steatohepatitis and metabolic syndrome in the Ossabaw miniature swine. Hepatology. 2009; 50:56–67. [PubMed: 19434740]
45. Libby P. Murine “Model” Monotheism: An Iconoclast at the Altar of Mouse. Circ Res. 2015; 117:921–925. [PubMed: 26541681]
46. Lipskaia L, Hulot JS, Lompre AM. Role of sarco/endoplasmic reticulum calcium content and calcium ATPase activity in the control of cell growth and proliferation. Pflugers Arch. 2009; 457:673–685. [PubMed: 18188588]
47. Lopes GS, Ferreira AT, Oshiro ME, Vladimirova I, Jurkiewicz NH, Jurkiewicz A, Smaili SS. Aging-related changes of intracellular Ca2+ stores and contractile response of intestinal smooth muscle. Exp Gerontol. 2006; 41:55–62. [PubMed: 16343836]
48. Lundberg MS, Curto KA, Bilato C, Monticone RE, Crow MT. Regulation of vascular smooth muscle migration by mitogen-activated protein kinase and calcium/calmodulin-dependent protein kinase II signaling pathways. J Mol Cell Cardiol. 1998; 30:2377–2389. [PubMed: 9925373]
49. Marijic J, Li Q, Song M, Nishimaru K, Stefani E, Toro L. Decreased expression of voltage- and Ca(2+)-activated K(+) channels in coronary smooth muscle during aging. Circ Res. 2001; 88:210–216. [PubMed: 11157674]
50. McKenney-Drake ML, Rodenbeck SD, Owen MK, Schultz KA, Alloosh M, Tune JD, Sturek M. Biphasic alterations in coronary smooth muscle Ca2+ regulation in a repeat cross-sectional study of coronary artery disease severity in metabolic syndrome. Atherosclerosis. 2016; 249:1–9. [PubMed: 27062403]

51. McKenney-Drake ML, Territo PR, Salavati A, Houshmand S, Persohn S, Liang Y, Alloosh M, Moe SM, Weaver CM, Alavi A, Sturek M. ^{18}F-NaF PET imaging of early coronary artery calcification. JACC Cardiovasc Imaging. 2016; 9:627–628. [PubMed: 26189122]
52. McKenney ML, Schultz KA, Boyd JH, Byrd JP, Alloosh M, Teague SD, Arce-Esquivel AA, Fain JN, Laughlin MH, Sacks HS, Sturek M. Epicardial adipose excision slows the progression of porcine coronary atherosclerosis. J Cardiothorac Surg. 2014; 9:2–12. [PubMed: 24387639]
53. Moon SK, Thompson LJ, Madamanchi N, Ballinger S, Papaconstantinou J, Horaist C, Runge MS, Patterson C. Aging, oxidative responses, and proliferative capacity in cultured mouse aortic smooth muscle cells. American Journal of Physiology: Heart and Circulatory Physiology. 2001; 280:H2779–H2788. [PubMed: 11356636]
54. Neeb ZP, Edwards JM, Alloosh M, Long X, Mokelke EA, Sturek M. Metabolic syndrome and coronary artery disease in Ossabaw compared with Yucatan swine. Comp Med. 2010; 60:300–315. [PubMed: 20819380]
55. Newell-Fugate AE, Taibl JN, Clark SG, Alloosh M, Sturek M, Krisher RL. Effects of diet-induced obesity on metabolic parameters and reproductive function in female Ossabaw minipigs. Comp Med. 2014; 64:44–49. [PubMed: 24512960]
56. Nilsson J, Sjolund M, Palmberg L, Von Euler AM, Jonzon B, Thyberg J. The calcium antagonist nifedipine inhibits arterial smooth muscle cell proliferation. Atherosclerosis. 1985; 58:109–122. [PubMed: 3004518]
57. Osler, W. The principles and practice of medicine : designed for the use of practitioners and students of medicine. Vol. xvi. Vol. 1079. New York: D. Appleton and Company; 1892. p. 2p. 1077-1078.
58. Owens GK, Kumar MS, Wamhoff BR. Molecular regulation of vascular smooth muscle cell differentiation in development and disease. Physiol Rev. 2004; 84:767–801. [PubMed: 15269336]
59. Pauly RR, Bilato C, Sollott SJ, Monticone R, Kelly PT, Lakatta EG, Crow MT. Role of calcium/calmodulin-dependent protein kinase II in the regulation of vascular smooth muscle cell migration. Circulation. 1995; 91:1107–1115. [PubMed: 7850948]
60. Phillips-Eakley AK, McKenney-Drake ML, Bahls M, Newcomer SC, Radcliffe JS, Wastney ME, Van Alstine WG, Jackson G, Alloosh M, Martin BR, Sturek M, Weaver CM. Effect of high-calcium diet on coronary artery disease in Ossabaw miniature swine with metabolic syndrome. JAHA. 2015; 4
61. Rich MW, Chyun DA, Skolnick AH, Alexander KP, Forman DE, Kitzman DW, Maurer MS, McClurken JB, Resnick BM, Shen WK, Tirschwell DL. American Heart Association Older Populations Committee of the Council on Clinical Cardiology CoC, Stroke Nursing CoCS, Anesthesia Stroke C, American College of C, American Geriatrics S. Knowledge Gaps in Cardiovascular Care of the Older Adult Population: A Scientific Statement From the American Heart Association, American College of Cardiology, and American Geriatrics Society. J Am Coll Cardiol. 2016; 67:2419–2440. [PubMed: 27079335]
62. Rodenbeck SD, Zarse CA, McKenney-Drake ML, Bruning RS, Sturek M, Chen NX, Moe SM. Intracellular calcium increases in vascular smooth muscle cells with progression of chronic kidney disease in a rat model. Nephrol Dial Transplant. 2017; 32:450–458. [PubMed: 27510531]
63. Sawabe M. Vascular aging: from molecular mechanism to clinical significance. Geriatrics & gerontology international. 2010; 10(Suppl 1):S213–220. [PubMed: 20590836]
64. Shah M, Sikkel MB. Coronary artery disease and age: beyond atherosclerosis. J Physiol. 2013; 591:5807–5808. [PubMed: 24293531]
65. Sturek M. Ca^{2+} regulatory mechanisms of exercise protection against coronary artery disease in metabolic syndrome and diabetes. J Appl Physiol. 2011; 111:573–586. [PubMed: 21596923]
66. Sturek, M., Tune, JD., Alloosh, M. Ossabaw Island miniature swine: metabolic syndrome and cardiovascular assessment. In: Swindle, MM., editor. Swine in the Laboratory: Surgery, Anesthesia, Imaging, and Experimental Techniques. Boca Raton: CRC Press; 2015. p. 451-465.
67. Taddei S, Virdis A, Mattei P, Ghiadoni L, Gennari A, Fasolo CB, Sudano I, Salvetti A. Aging and endothelial function in normotensive subjects and patients with essential hypertension. Circulation. 1995; 91:1981–1987. [PubMed: 7895356]

68. Teoh H, Man RYK. Enhanced relaxation of porcine coronary arteries after acute exposure to a physiological level of 17β-estradiol involves non-genomic mechanisms and the cyclic AMP cascade. British Journal of Pharmacology. 2000; 129:1739–1747. [PubMed: 10780981]
69. Trask AJ, Katz PS, Kelly AP, Galantowicz ML, Cismowski MJ, West TA, Neeb ZP, Berwick ZC, Goodwill AG, Alloosh M, Tune JD, Sturek M, Lucchesi PA. Dynamic micro- and macrovascular remodeling in coronary circulation of obese Ossabaw pigs with metabolic syndrome. J Appl Physiol (1985). 2012; 113:1128–1140. [PubMed: 22837170]
70. Tumbleson ME, Hicklin KW, Burks MF. Serum cholesterol, triglyceride, glucose and total bilirubin concentrations, as functions of age and sex, in Sinclair(S-1) miniature swine. Growth. 1976; 40:293–300. [PubMed: 976771]
71. Wamhoff BR, Bowles DK, McDonald OG, Sinha S, Somlyo AP, Somlyo AV, Owens GK. L-type voltage-gated Ca2+ channels modulate expression of smooth muscle differentiation marker genes via a rho kinase/myocardin/SRF-dependent mechanism. Circ Res. 2004; 95:406–414. [PubMed: 15256479]
72. Wang JC, Bennett M. Aging and atherosclerosis: mechanisms, functional consequences, and potential therapeutics for cellular senescence. Circ Res. 2012; 111:245–259. [PubMed: 22773427]
73. Wastney M, Lee W, Jackson GS, Alloosh M, Sturek M, Lachcik P, Peacock M, Martin B, Weaver CM. Soft tissue calcification in the Ossabaw miniature pig: experimental and kinetic modeling studies. Osteoporos Int. 2013; 24:2123–2126. [PubMed: 23224107]
74. Witczak CA, Wamhoff BR, Sturek M. Exercise training prevents Ca^{2+} dysregulation in coronary smooth muscle from diabetic dyslipidemic Yucatan swine. J Appl Physiol. 2006; 101:752–762. [PubMed: 16763107]
75. Woodward, SL., Quinn, JA. Encyclopedia of invasive species : from Africanized honey bees to zebra mussels. Santa Barbara, Calif: Greenwood; 2011. Feral Pig (Sus scrofa); p. 275-280.
76. Yildiz O. Vascular smooth muscle and endothelial functions in aging. Ann N Y Acad Sci. 2007; 1100:353–360. [PubMed: 17460198]
77. Yoshikawa A, Van Breemen C, Isenberg G. Buffering of plasmalemmal Ca^{2+} current by sarcoplasmic reticulum of guinea pig urinary bladder myocytes. American Journal of Physiology Cell Physiology. 1996; 271:C833–C841.
78. Yu E, Mercer J, Bennett M. Mitochondria in vascular disease. Cardiovasc Res. 2012; 95:173–182. [PubMed: 22392270]
79. Zhou RH, Vendrov AE, Tchivilev I, Niu XL, Molnar KC, Rojas M, Carter JD, Tong H, Stouffer GA, Madamanchi NR, Runge MS. Mitochondrial oxidative stress in aortic stiffening with age: the role of smooth muscle cell function. Arterioscler Thromb Vasc Biol. 2012; 32:745–755. [PubMed: 22199367]

Highlights

- We compared vascular health in both aged and metabolic syndrome (MetS) swine.
- Old lean swine had media thickening, while old MetS swine had intima thickening.
- Young and old MetS swine had Ca^{2+} handling that resembled severe coronary disease.
- Old lean swine had Ca^{2+} handling that resembled mild coronary disease.
- Aging milieu possibly caused more advanced plaques to develop in a MetS background.

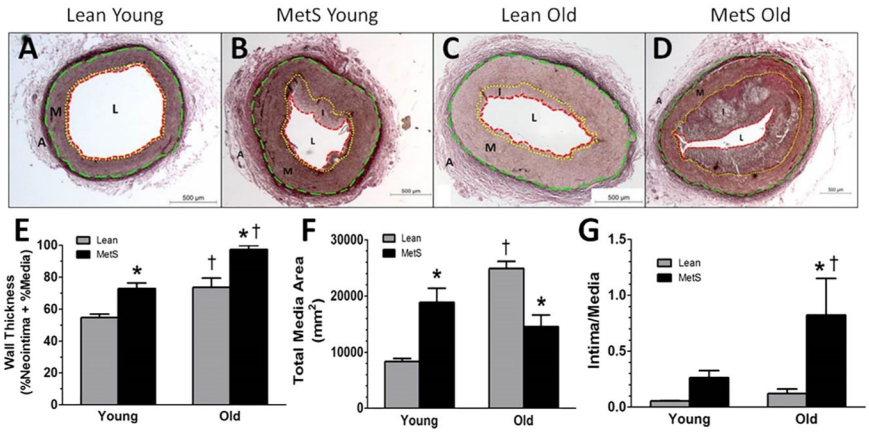

Figure 1. Histological staining reveals structural changes in MetS and old swine

Representative VVG histological stain of right coronary arteries reveals lean young swine (A) have almost no neointima formation. MetS young swine (B) and lean old swine (C) have similar media thickness. MetS old swine (D) had the most advanced neointimal thickening. (E) MetS young and lean old swine both have significantly greater wall thickness compared to lean young swine, and MetS old swine exhibited the most severe wall thickness. (F) MetS young and lean old swine both exhibit media thickening that is significantly greater compared to lean young swine. (G) MetS young swine trend towards a greater intima:media area ratio compared to lean young, and MetS old swine have a greater intima:media ratio than the other groups, indicating a greater contribution of neointimal growth to disease pathology. External elastic lamina = green dashed line; internal elastic lamina = yellow dotted line; lumen = red dashed line. A, adventitia; M, media (wall); I, intima (plaque); L, lumen. *, $p < 0.05$ compared with lean swine; †, $p < 0.05$ compared with young swine. (Lean young = 6; MetS young = 9; Lean old = 4; MetS old = 3.)

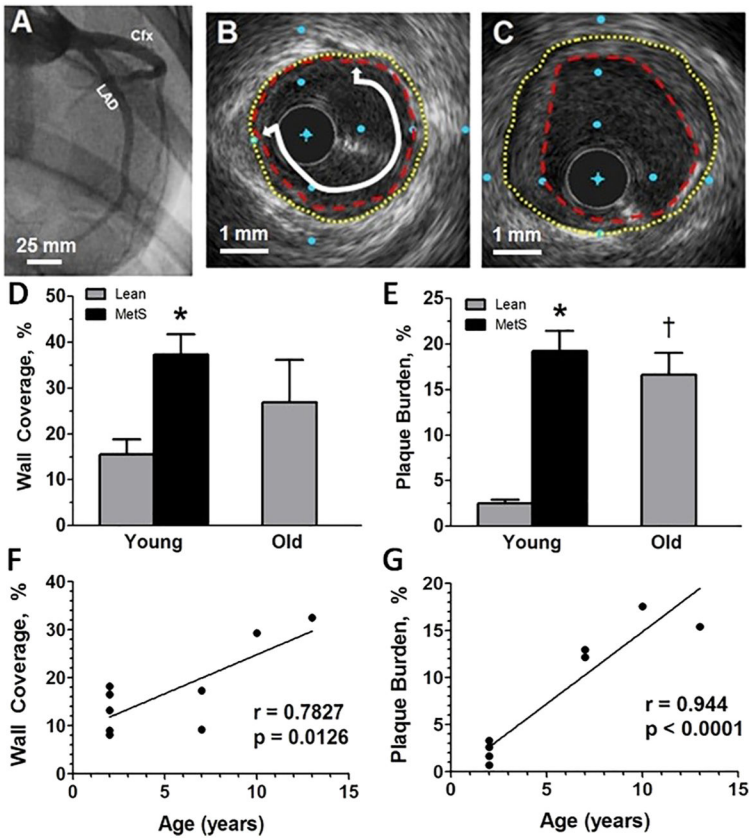

Figure 2. MetS young swine and lean old swine have comparable CAD severity as measured by intravascular ultrasound

(A) Angiogram showing the LAD and Cfx coronary arteries from a lean young swine. (B) Cross sectional view of a lean old swine with mild disease. (C) Cross sectional view of a MetS young swine with more severe disease. (D) MetS young swine have higher percent wall coverage than lean young swine in the proximal 15 mm of the LAD. (E) MetS young and lean old swine have greater percent plaque burden compared to lean young swine. Both percent wall coverage (F) and percent plaque burden (G) are positively correlated to age in lean swine. Original lumen = yellow dotted line; plaque encroachment = red dashed line; wall coverage = white line with arrows. The distance between blue dots in B and C is 1 mm. *, $p < 0.05$ compared with lean swine; †, $p < 0.05$ compared with young swine. (Lean young = 6; MetS young = 10; Lean old = 5; MetS old = 3)

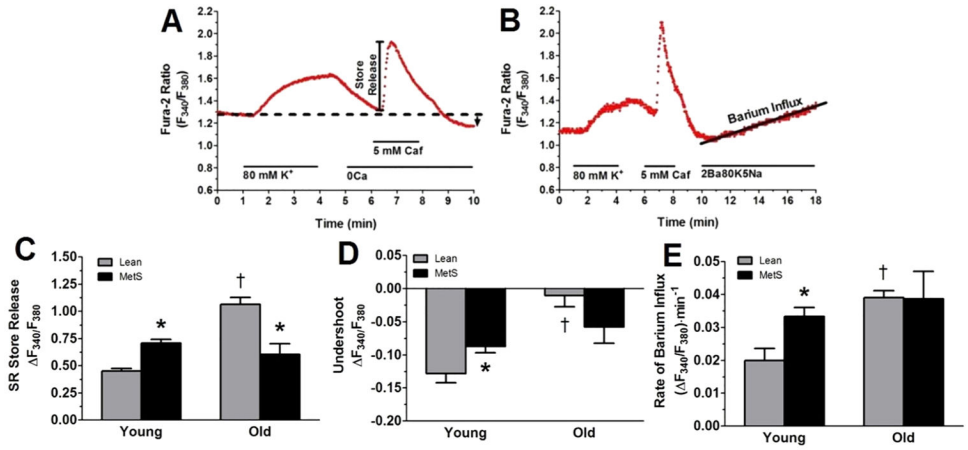

Figure 3. Ca^{2+} handling changes observed in MetS young and MetS old swine are exacerbated in old lean swine

(A) Representative tracing showing the change in the F_{340}/F_{380} excitation fluorescence emission ratio of a CSM cell isolated from a lean young swine. Treatments and duration are indicated by solid lines. Ca^{2+} influx was initiated by depolarization of the cell with an 80 mM K^+ solution, which maximally loaded the SR store. The 5 mM caffeine activated ryanodine receptors, causing total SR store release. After caffeine wash-out, the undershoot (black arrow), which is indicative of SERCA activity, was measured. (B) Representative tracing of a CSM cell isolated from a lean young swine and treated with a solution containing 2 mM Ba^{2+}, 80 mM K^+, and 5 mM Na^+ (2Ba80K5Na). Rate of barium entry is indicative of VGCC activity. Caf, caffeine. (C) Caffeine-induced SR store release was elevated in MetS young and lean old swine. (D) The undershoot, which is a direct measurement of SERCA function, was attenuated in MetS young and lean old swine (E) Increased Ba^{2+} influx was observed in the MetS young and lean old swine. *, $p < 0.05$ compared with lean swine; †, $p < 0.05$ compared with young swine. (Lean young = 6; MetS young = 10; Lean old = 4; MetS old = 3.)

Table 1

Ossabaw Swine Cardiometabolic Characteristics.

	Lean Young	MetS Young	Lean Old	MetS Old
Age (years)	2.0 ± 0.0	2.5 ± 0.2	9.2 ± 1.1 *†	8.8 ± 1.2 *†
Body Weight (kg)	74 ± 4	108 ± 2 *	87 ± 5 †	113 ± 7 *‡
Sex (Male/Female)	2/4	0/10	3/2	0/3
Total Cholesterol (mg/dL)	77 ± 6	474 ± 79 *	60 ± 4 †	411 ± 66 ‡
Triglycerides (mg/dL)	65 ± 18	56 ± 5	17 ± 4 *†	20 ± 6
Fasting Glucose (mg/dL)	70 ± 2	81 ± 2	52 ± 12 †	78 ± 7
Peak Glucose (mg/dL)	563 ± 27	755 ± 22 *	688 ± 20	733 ± 44 *
Blood Glucose AUC	10120 ± 667	18124 ± 919 *	12237 ± 464 †	15297 ± 1556 *

Data are means ± SEM. MetS, metabolic syndrome; MAP, mean arterial pressure; AUC, area under curve. Fasting glucose was taken during intravenous glucose tolerance tests or during routine blood glucose monitoring for the lean old group.

* $p < 0.05$ compared with young lean swine;

† $p < 0.05$ compared with young MetS swine;

‡ $p < 0.05$ compared with old lean swine.

The n-values of males and females for all groups applies to all Figures 1–3. (Lean young = 6; MetS young = 10; Lean old = 5; MetS old = 3)